Assembly of Effective Halide Receptors from Components. Comparing Hydrogen, Halogen, and Tetrel Bonds

Steve Scheiner*
Department of Chemistry and Biochemistry
Utah State University
Logan, UT 84322-0300

*email: steve.scheiner@usu.edu
phone: 435-797-7419

ABSTRACT

Receptors for halide anions are constructed based on the imidazolium unit, and then replacing the H-bonding C-H group first by halogen-bonding C-I and then by tetrel-bonding C-SnH_3 and C-SiF_3. Attaching a phenyl ring to any of these species has little effect on its ability to bind a halide, but incorporation of a second imidazolium to the benzene connector, forming a bidentate dicationic receptor, greatly enhances the binding. Addition of electron-withdrawing F atoms to each imidazolium adds a further increment. F^- consistently binds more strongly to the various receptor models than does Cl^-. Whereas replacement of the H atom on the imidazolium groups with the halogen-bonding I has an inconsistent perturbing effect, tetrel-bonding SnH_3 significantly enhances the binding with either halide, and SiF_3 even more so. Placement of the various complexes into aqueous solution reduces binding energies, but the trends that occur in the gas phase are largely reproduced in water. The tetrel-bonding receptors are the most selective for F^- over Cl^-, with an equilibrium ratio on the order of 10^{14} for SnH_3 and 10^{28} for SiF_3 . When combined with their strong halide binding, SiF_3-ImF_3-Bz-ImF_3-SiF_3^{+2} bipodal receptors represent an optimal choice in terms of both binding strength and selectivity.

INTRODUCTION

The detection, extraction, and transport of anions is of paramount importance in a wide diversity of applications, whether biological or chemical, medical or environmental [1]. In the biological realm, various organisms have evolved binders that are highly specific for one anion or another. One example is the sulphate-binding protein of Salmonella typhimurium [2] which binds this anion via a number of H-bonds. Another protein is responsible for the binding and transport of phosphate [3] with very high specificity. There is a protein in blue-green algae that is highly specific for the nitrate anion [4], and another binds specifically to bicarbonate [5]. Whereas the evolutionary process has developed some very specific and selective anion binding agents, modern technology lags behind. Many receptors make use of general electrostatic interactions, and sometimes of H-bonds [6-8]. The thiourea molecule, for example, is a widely used [9-12] anion binder, taking advantage of its H-bonding capability.

One important advance in this field has arisen with the growing recognition of the phenomenon of halogen bonds (XBs) [13-19], wherein an attractive force occurs between a halogen atom and an electron donor, such as the lone pair of an amine. One of the more intriguing and potentially useful applications of XBs is associated with the development of receptors that are highly selective for one anion over another [20-32]. Our own group [33-35] has applied quantum chemical calculations to this issue, showing that the replacement of H in a series of H-bonding bidentate receptors by halogen atoms can indeed enhance their binding to halides. The work detailed a remarkable enhancement of both binding and selectivity, most particularly when the H atom is replaced by I.

It seems clear, then, that halogen bonding has enormous potential to magnify the ability of receptors to bind anions. But just as the switchover from H to halogen bonding introduced a new dimension to the field, extending this same philosophy to other related sorts of bonding may also offer added benefits. More specifically, just as the elements of the halogen family (Cl, Br, I, etc) can replace H as a bridging atom in strongly bound complexes, the same is equally true for other families in the periodic table. There is rapidly growing evidence, for example, that chalcogen atoms such as S and Se engage in bonding of a parallel sort [36-42]. And indeed that chalcogen bonds can act to bind various anions to receptors has already been well documented [43-47].

These sorts of binding patterns are not limited to halogens and chalcogens, but are widely reported as well for pnicogens (P, As, etc) [48-56]. Although not as well documented at this juncture, there is a growing avalanche of data that demonstrate the same is true of tetrels (Si, Ge, etc) [57-65]. These notions should not be entirely surprising, as all of these atoms, like halogens, display highly asymmetric charge distributions when bound to another atom, and are even less electronegative than the halogens, so have a better native ability to generate a positive electrostatic potential region directed toward an approaching nucleophile.

It was just this idea that motivated our group to perform a set of calculations to examine how the latter sorts of bonds might compare with one another in this context. The transition from chalcogen to pnicogen to tetrel yielded [66] not only progressively stronger binding to anions, but also greater selectivity. In a quantitative sense, the binding energy of halides to a tetrel-bonding bidentate receptor was as high as 63 kcal/mol, and preferentially bound F^- over other halides with a selectivity of 27 orders of magnitude. These quantities are especially impressive, given the fact that the receptor was electrically neutral, forgoing the positive charge on many other such candidates. These findings were reinforced [67] by additional calculations that showed an enhancement when progressing further down each column of the periodic table.

In an interesting distinction, whereas the strongest fluoride binding agents utilize the tetrel bonds of the Sn atom, it is I-halogen bonds that are preferred for Cl^- and Br^-.

The aforementioned calculations, and many of the experimental measurements, have centered on bipodal receptors in which a pair of imidazoliums act as the direct binding units. These two rings are attached to one another through the intermediacy of a relatively inert connecting unit, in many cases a benzene ring. The past findings lead to several important questions related to the design and synthesis of effective anion binding agents. In a general sense, do the various parts of the receptors work in concert with one another; i.e. is the whole greater than the sum of its parts? More specifically, are two binding agents on the same molecule truly better than one? Does the binding suffer, and if so by how much, if the bipodal receptor is replaced by the much simpler single imidazolium? What is the influence of the connecting benzene ring; does the binding of an imidazolium improve if attached to such a ring? Since it is well known that the proximity of electron-withdrawing agents add to the electron-accepting ability of a Lewis acid, can the full receptor be improved by adding such agents onto the imidazolium rings? Past work has suggested that tetrel bonding compares favorably with both halogen and hydrogen bonding, so a comparison of these three binding modes is in order. It should be stressed that an effective binding agent is not defined simply by the strength of its interaction with a halide, but also by its degree of selectivity for one anion over another. So the data below focus on both of these two issues.

SYSTEMS AND METHODS

The dimethyl-imidazolium ion ImH^+ was taken as a starting point for complexation with halides F^- and Cl^-. These two anions are used in order to measure selectivity for one anion over the other, as past work [33-35, 66-67] has indicated a great deal of differential binding between the two of them. As illustrated in Figs 1a and 1b, these halides interact directly with the CH group that lies between the two methyl groups. In order to assess any enhancement in binding that arises by changing the bonding from a H-bond (HB) to halogen or tetrel bond, this central H was changed respectively to I and SnH_3, as displayed in Fig 1. These atoms were chosen from the fourth row of the periodic table as past results [66-67] suggest they form especially strong halogen and tetrel bonds, respectively. On the other hand, it is widely understood that the addition of electron-withdrawing agents enhances the ability of the atom in question to accept electrons. So even though Si lies two rows higher than Sn in the periodic table, and thus forms weaker tetrel bonds, its Lewis acid strength ought to be enhanced by adding F atoms. Consequently, it is of interest to compare the binding of SnH_3 with SiF_3, also pictured in Fig 1.

The first step in formation of the bidentate receptors that contain a pair of imidazoliums is the addition of a benzene ring connector, so the methyl group on one N atom was replaced by a phenyl group, as pictured in Fig 1c. The full bidentate receptor is achieved when a second ImH^+ is added to the phenyl ring, with structures of the dications illustrated in Fig 2. As in the monodentate cases, the CH group of each ImH^+ was replaced alternately by I, SnH_3, and SiF_3. In keeping with the observation that the presence of electron-withdrawing agents near the electrophile enhance the binding, a single F atom was added to each of the two Im rings, ortho to the electrophilic group, as indicated in Fig 3. This effect was magnified by adding two more F atoms, for a total of three, on each ring, shown diagrammatically in Fig 4. Each of these receptors was paired with both F^- and Cl^-, for a total of 36 different receptor-halide pairs. The imidazoliums and benzene spacer groups were chosen first because of their resemblance to receptors studied earlier [1, 8, 21, 28, 47, 68-71], and also because prior calculations [35] had indicated they represent an optimal choice for this purpose.

All the calculations were carried out with the M06-2X DFT functional [72] in conjunction with the aug-cc-pVDZ basis set, within the framework of the Gaussian-09 [73] set of codes. For the heavy atoms I and Sn, the aug-cc-pVDZ-PP pseudopotential was taken directly from the EMSL library [74-75] so as to incorporate relativistic effects. This level of theory is appropriate for this task, as evident by previous work by others [76-85] and very recently by ourselves in dealing with very similar sorts of systems [33-35]. The geometries of the receptors and complexes were fully optimized without any restriction, taking into account only true minima with all positive vibrational frequencies. The binding energy, E_b, of each halide with its receptor was calculated as the difference between the energy of the complex and the sum of the energies of separately optimized monomers. Each binding energy was corrected for basis set superposition error using the counterpoise [86] procedure. To account for solvent effects, the polarizable conductor calculation model (CPCM) was applied [87], with water as the solvent. Molecular electrostatic potential maps were visualized and quantified with the Chemcraft and WFA-SAS programs [88-89] and charge transfer assessed via the Natural Bond Orbital (NBO) technique [90].

RESULTS

The optimized geometries of ImH^+ and its I, SnH_3, and SiF_3-substituted derivatives with F^- and Cl^- are illustrated in Fig 1a and 1b, respectively. The ImI^+ complexes are linear around the I atom, while some deviations from linearity are observed in the H, SnH_3, and SiF_3 structures. The largest deviation occurs when ImH^+ is paired with Cl^-, as a secondary CH••Cl HB, of length 2.591 Å is formed with one of the two methyl groups. However, this HB is obviously quite a bit weaker, longer and more bent, than the primary interaction with the central CH of imidazolium. It is also notable that this same CH proton effectively transfers to F^-, lying much closer to F than to C. The I, SnH_3, and SiF_3 groups also lie closer to F than to the imidazolium C. Such a transfer does not occur in the Cl^- analogues. Whether F^- or Cl^-, the halide lies somewhat closer to Sn than it does to I, by 0.08-0.10 Å, with the Si··X distance shorter still.

The binding energies of the F^- and Cl^- anions to the receptors are recorded in the first two rows of Table 1. It is immediately clear that the former binds much more strongly than the latter, by a factor of 4 to 5. This strengthening is due first to the higher charge concentration of F^-. A second factor is the near transfer of the R group from the imidazole ring to F, as r(R-F) is consistently shorter than is r(R-C). The Sn atom serves as a stronger anchor to the halide, followed by H and then by I, although the latter two are reversed when F^- is changed to the larger Cl^-. It is the perfluorinated SiF_3 group, however, that engages in the strongest binding of all.

In construction of the bipodal receptors, a phenyl ring is attached directly to one of the N atoms of the imidazolium. Such a ring therefore was substituted for one of the two methyl groups, and the optimized geometries of these modified imidazoliums with F^- are illustrated in Fig 1c. It is immediately apparent that the methyl-to-phenyl mutation affects the analogous geometries of Fig 1a in only minor ways. In either case, the R group transfers across to F. And the mutation effect on the binding energies is vanishingly small, below 3%.

The next step in construction of the bipodal receptors is the placement of a second imidazolium ring on the connecting phenyl. Figs 2a and 2b display the optimized geometries of the H, I, Sn, and Si receptors, when bound respectively to F^- and Cl^-. The geometries are symmetric, or very nearly so, with the halide equally distant from the two R groups. Unlike the single Im rings in Fig 1, there is no transfer of either the H or I atoms to F, although the SnH_3 groups are roughly halfway transferred, with r(Sn-F) slightly shorter than r(Sn-C); similarly for SiF_3. In comparison to the monodentate complexes in Fig 1, r(C-R) is shorter

and r(R-X) is longer. Any strain involved in forming a pair of bonds to the halide is largely muted, with θ(C-R-X) angles between 156° and 171° in the bidentate species of Fig 2. With respect to the orientation of the central phenyl ring it lies nearly in the plane of the two imidazole rings for R=H, but more nearly perpendicular for R=I and SnH_3.

The energetics of these bipodal complexes are contained in the R-Im-Bz-Im-R^{+2} rows of Table 1. Not surprisingly, these quantities are considerably larger than the corresponding monodentate energies. This magnification is equal to a factor of 1.5 for X=F, but larger for X=Cl, between 2.0 and 3.9. In a sense, then, the binding to Cl^- is cooperative in that the formation of two R••Cl bonds is more than twice as strong as the single bond for the monodentate receptors. In contrast, the binding to F^- is anticooperative as the bipodal receptors bind less than twice as strongly as do their monopodal analogues. In the context of the bidentate species, the smaller F^- is bound roughly twice as strongly as is Cl^-, not quite as extreme a difference as monodentate.

It is well known that adding electron-withdrawing agents in the vicinity of the electron-accepting R unit will typically enhance the ability of this species to engage with an electron donor such as a halide anion. A F atom was thus added to each of the two imidazolium rings, as depicted in Fig 3. The effects of this substitution can be recognized by comparison to the unsubstituted complexes in Fig 2. In the case of R=H, the substitution moves the F^- to an asymmetric position, along with a transfer of one of the CH protons to it, with r(FH)=1.004 Å. There is also a loosening up of the CH••O HB to the phenyl ring, with r(H••F) elongating from 2.033 to 2.240 Å. The effects on the Cl^- binding geometry are more minor, although the HB to the central phenyl group is broken. For R=I, SnH_3, and SiF_3, the H-to-F mutation simply shortens the R••X distances, with accompanying smaller elongations of the covalent C-R bonds. The addition of two more F atoms on each Im ring introduces only minor further perturbations of the geometry. Comparison of these hexa-substituted F receptors in Fig 4 shows further reductions in the R••X distances, and smaller elongations of the C-R covalent bonds.

The last four rows in Table 1 report the energetics of the F-substituted receptors. One sees that these substitutions lead to progressive enhancements in the binding energy. The first pair of F mutations raise this quantity by 11-16 kcal/mol for F^- and 7-18 for Cl^-; the increments for the next four F substitutions are a bit smaller, roughly 65% of those arising from the first pair of F replacements. Considering the full results in Table 1 in total, one sees first of all that the tetrel bonding for R=SnH_3 is consistently stronger than for H or I, and that for the fluorinated tetrel SiF_3 stronger still. Indeed, the latter binding represents an increment of some 25 kcal/mol (12%) over SnH_3 for F^-, and as much as 16 kcal/mol for Cl^-. F^- binds much more strongly than does Cl^-. The largest binding energy of all, 251 kcal/mol, is associated with F^- and the hexafluorinated receptor with R=SiF_3.

Aqueous Environment

A great deal of interest lies in the use of anion receptors within an aqueous environment. Accordingly, the binding energies of the various complexes were computed when the system was immersed in water, within the context of the CPCM protocol which views solvent as a polarizable medium. Since the individual participants are both electrically charged, the receptor is a mono/dication and the halide a monoanion, this medium very strongly stabilizes the separated monomers, much more so than the complex with an overall charge of 0 or +1. Consequently, the binding energies are greatly reduced, as may be seen in Table 2 in which these quantities are compiled. Despite these reductions, the trends remain quite similar to those in the gas phase, as is evident by a comparison of Fig 5b with 5a. Regardless of medium, the

fluoride (solid lines) is bound more strongly than chloride (broken lines). As one moves from left to right in Fig 5, the single Im ring is replaced by a pair of rings, then first 1 and then 3 F atoms are added to each ring. Regardless of medium, each of these changes produces an enhancement in the binding. With respect to the F^- solid lines, R=SnH_3 which is denoted by red lines, binds more strongly than do R=H (black) or I (purple). This latter distinction is most obvious for aqueous solution, where R=I binds more strongly than does R=H. The green lines associated with the SiF_3 perfluorinated tetrel substituents are considerably higher than all others. This large increment is particularly notable for fluoride binding in water. Chloride binding is less dependent upon R, although R=H is noticeably more weakly bound for the fluorinated Im rings in water. It is stressed finally that despite the ability of aqueous solution to weaken the interaction, the binding energies remain rather large, particularly for fluoride, where E_b ranges up to as high as 64 kcal/mol.

By suitable incorporation of vibrational and entropic effects, one can compute the free energies of binding. These quantities are generally a bit less exothermic than are ΔE, generally by some 5-11 kcal/mol. More importantly, these changes are fairly uniform from one system to the next, and so the trends in Fig 5 are basically unaltered. For example, the free energy of the most strongly bound complex between SiF_3-ImF_3-Bz-ImF_3-SiF_3^{+2} and F^- is 238 kcal/mol in the gas phase, less exothermic than ΔE by some 13 kcal/mol. As another example, the binding energy of Cl^- with H-Im-Bz-Im-H^{+2} is 98 kcal/mol, reduced to 90 kcal/mol when ΔG is evaluated.

As mentioned earlier, F^- is bound more strongly than is Cl^-, so these receptors are capable of a certain degree of selectivity for the former over the latter. The free energy advantage of binding of fluoride over chloride is contained in Table 3 where it may be seen to vary from a minimum of 8.7 kcal/mol for Im-H^+ to as high as 40 kcal/mol for SiF_3-ImF-Bz-ImF-SiF_3^{+2}. Indeed, the R= SiF_3 receptors in the last column of Table 3 show the largest ΔG selectivity of 37-40 kcal/mol, roughly twice that of even the SnH_3 analogues. The equilibrium ratio of fluoride to chloride bound receptors can be expressed as K=exp(ΔG{F^-}-ΔG{Cl^-})/RT which are displayed in the indicated rows of Table 3. Clearly, the R=SiF_3 receptors are uniformly the most selective, with K~10^{28}. They are followed by their SnH_3 sisters with quantities of roughly 10^{14}. The R=I receptors are much less selective, with K in the range between 10^7 and 10^8. There is a good deal of variability for R=H. If the Im rings are not fluorinated K is roughly 10^6 - 10^7, but this quantity rises as F atoms are added to the Im rings, reaching $4x10^{11}$ for a single F atom, and as much as $5x10^{14}$ for trisubstituted rings.

An optimal receptor will not only be selective for F^-, but will also bind it strongly. So while H-ImF_3-Bz-ImF_3-H^{+2} shows a selectivity comparable to its SnH_3-substituted analog, Table 2 shows the binding energy of the former is 29 kcal/mol, compared to 41 kcal/mol for SnH_3-ImF_3-Bz-ImF_3-SnH_3^{+2}. This 12 kcal/mol difference corresponds to nearly a 10^9 advantage when expressed as a Boltzmann ratio. But the SiF_3 tetrel binding receptors are superior in both respects. Not only is their equilibrium F^-/Cl^- ratio much larger than any of the others, but their binding energy is also the greatest, and by a wide margin. In summary, the R= SiF_3 receptors show the highest selectivity for F^- over Cl^-. When coupled with a pair of trifluorinated Im rings, the combination of strong binding and high selectivity make these receptors the optimal choice.

Electronic Structure Analysis

There are a number of measures of noncovalent bond strength that derive from analysis of the wave function. One of these measures is associated with the natural bond orbital (NBO) approach which

evaluates energetic contributions of charge transfers from one localized orbital to another. In the systems being considered here, the most prominent such charge transfer is that from the occupied lone pairs of the halide to the σ*(C-X) antibonding orbital of the substituted imidazolium. These quantities are displayed in the first four columns of Table 4. In a number of cases, particularly those involving the SnH_3 substituent, the Sn atoms are nearly equally distant between the halide and the imidazole, i.e. there is at least partial Sn transfer, which complicates the NBO analysis which depends upon a clear separation. One can nonetheless see certain enlightening trends in the NBO data. For example, the monodentate complexes in the first two rows show evidence of a stronger X••R interaction than the bidentate systems which involve two, albeit weaker, such noncovalent bonds. The inclusion of first two and then six F atoms on the imidazolium pair adds to the charge transfer, parallel to the bonding trends in Tables 1 and 2. On the other hand, even though F^- is consistently bound more strongly than is Cl^-, there is only a small margin between the two with respect to E(2), although this comparison is clouded somewhat by the tendency of the H of the unsubstituted imidazolium to transfer to the former halide. The R=SiF_3 values do reflect the stronger binding of F^- over Cl^-, but not in the monocation cases.

The issue of partial transfer is less problematic in the AIM analysis of the wave function. The total density at the pertinent bond critical point between X^- and the R atom is reported in the last four columns of Table 4. One can see first of all that these densities are larger for the F••R noncovalent bonds as compared to Cl••R. As in the case of E(2), the single X••R bond in the monodentate complexes are stronger than each of the individual such bonds in their bidentate sisters. Like the interaction energies themselves, ρ_{BCP} does not show much variation with respect to the choice of binding atom R, although SiF_3 is consistently largest. There is again the clear tendency that progressive F-substitution on the imidazolium rings enhances the noncovalent bond strength.

Due to the fact that a full charge is carried by both partners in each complex, it seems obvious that a good deal of the interaction will arise from simple Coulombic attraction. One can assess the readiness of each receptor to an incoming anion by inspection of the molecular electrostatic potential (MEP) that surrounds it. Indeed, prior work [44] has shown that the MEP can correlate quite nicely with experimental anion binding in related systems. In particular, the area between the two R groups where the halide is destined to reside is of greatest interest. This potential is illustrated for the various receptors in Fig 6. Due to the positive overall charge on the receptor, the potential is positive over the entire surface; the red and blue regions respectively indicate the least and most positive areas. The single positively charged receptors in the top row quite naturally have a lower potential overall than do the dications, so a different set of extrema is used to show the full range. Also, the R=H receptors tend to have a more positive surrounding potential than the other R groups.

It appears that the R=I, SnH_3, and SiF_3 groups are not the most positive regions, but that there is a more prevalent blue color around the remainder of the Im ring. For R=H, on the other hand, the most positive area surrounds the C-H proton(s). It is therefore not unreasonable to suspect that an anion might prefer a location other than that targeted in this work. To test this notion, both F^- and Cl^- anions were allowed to approach several of the imidazolium species from a number of different directions. Taking the ImI^+ imidazolium as a test case, a fluoride was placed initially in a position where it might approach one of the methyl groups head-on which could facilitate the formation of a trifurcated CH••F H-bond. The fluoride was also placed directly above the Im ring, above the two C atoms that are bonded to H rather than methyl groups. In either case, the F^- moved so as to displace the I atom from the C-I group, taking advantage of

the energetic preference for a covalent C-F over a C-I bond, as well as the instability of the very compact F^- anion as compared to the much more diffuse I^-. Such structures do not represent receptor/halide configurations. When placed initially in the plane of the ImI^+, approaching its two CH bonds, the F^- extracted one of these two protons, forming a neutral FH molecule; this arrangement was less stable than the halogen-bonded species by some 9.8 kcal/mol.

Unlike F^-, Cl^- is unable to replace the I atom on ImI^+. It will engage in a H-bonded complex with one of the two methyl groups, but this structure is 20.7 kcal/mol higher in energy than the halogen-bonded complex. Cl^- will also form CH••Cl H-bonds with the two CH groups of ImI^+, but again less stable than the CI••Cl structure, this time by 17.4 kcal/mol. Chloride also can find itself above the ImI^+ plane, specifically 2.81 Å above the C atom bonded to I; this local minimum is 4.5 kcal/mol less stable than the halogen bond of interest. With respect to the diimidazolium I-Im-Bz-Im-I^{+2}, a fluoride can position itself on the other side of the receptor from the I atom, engaging in CH••F HBs, but this minimum lies 13.9 kcal/mol higher in energy than the halogen-bonded global minimum. When placed initially over the plane of one of the two ImI rings, the F^- anion will again displace one of the two I atoms. In summary, then, the halogen-bonded species discussed above do indeed represent the global minima for noncovalent binding of the halides.

Another view of the electrostatic potential focuses on its value at a particular point in space. The point chosen is traditionally that which corresponds to the maximum of the potential on a surface surrounding the molecule that represents a constant electron density of 0.001 au. The value of this quantity, commonly referred to as $V_{s,max}$ for each receptor is displayed in Table 5. The maximum chosen in each case is that which most closely represents the position to be adopted by the incoming halide, roughly along the extension of the C-R axis. Like the full maps of the potentials in Fig 6, the values of $V_{s,max}$ are more positive for the dications than for the monocations in the first row of Table 5. A second trend is the much higher values for R=H and SiH_3, followed by SnH_3 and then I, as in the sequence H ~ SiF_3 >> SnH_3 > I. Note also that each substitution of additional F atoms on the Im rings also adds to the magnitude of $V_{s,max}$, as one progresses down each column of Table 5.

There are certain trends in $V_{s,max}$ that mimic those observed for the binding energies. For example, the stronger binding of SiF_3 over SnH_3 and then over I is correctly predicted by $V_{s,max}$. The stronger binding caused by progressive fluorosubstitution is also observed in both quantities. On the other hand, while R=H has the highest $V_{s,max}$, its binding energy is typically less than that observed for R=SiF_3 and SnH_3, and even R=I in certain cases. One might conclude that while the electrostatic potential certainly offers important clues as to the ability of a given receptor to bind to a halide, it cannot be taken as an absolute predictor of relative binding strength.

SUMMARY AND DISCUSSION

F^- consistently binds more strongly to the various receptor models than does Cl^-. The addition of a phenyl ring to a single imidazolium perturbs the binding very little. On the other hand, placement of a second imidazolium on the benzene connector group markedly enhances binding energies. Although less than a full doubling for F^- binding, there is a strong cooperative effect for Cl^- which more than doubles E_b. Whereas replacement of the H atom on the imidazolium groups with the halogen-bonding I has an inconsistent perturbing effect, tetrel-bonding SnH_3 significantly enhances the binding with either halide, and this effect is even stronger for SiF_3. The addition of electron-withdrawing F substituents on the Im rings adds a substantial increment to the binding energies.

Placement of the various complexes into aqueous solution reduces binding energies, due to the preferential stabilization by the medium of the oppositely charged separated species, as compared to the complexes. Nevertheless, the trends in binding energy that occur in the gas phase are reproduced in water, barring several minor perturbations. These same trends are true also when binding energetics are converted to free energies by inclusion of vibrational and entropic effects. The tetrel-bonding receptors are the most selective for fluoride over chloride, with an equilibrium ratio on the order of 10^{14} for SnH_3 and 10^{28} for SiF_3. When combined with their strong halide binding, SiF_3-ImF_3-Bz-ImF_3-SiF_3^{+2} bipodal receptors represent an optimal choice in terms of both binding strength and selectivity.

There are certain facets of the conclusions arising from the calculations that are consistent with prior experimental measurements. For example, the magnification of binding energy noted here when a single receptor group such as imidazolium or its substituted analogs is combined with a second such group in a bipodal arrangement is consistent with a recent experimental report [45] of a ten-fold magnification of binding constant with halides. Moreover, there is every reason to think that the computed values of ΔG in solution might closely reproduce experimental quantities, based in part on the good agreement noted earlier [44] for the chalcogen bonds formed by Te with halides. There has also been a good correlation noted [91] between binding sensitivity and ΔH.

REFERENCES

1. Langton, M. J.; Serpell, C. J.; Beer, P. D. Anion Recognition in Water: Recent Advances from a Supramolecular and Macromolecular Perspective. *Angew. Chem. Int. Ed.* **2016,** *55*, 1974-1987.
2. Pflugrath, J. W.; Quiocho, F. A. Sulphate Sequestered in the Sulphate-Binding Protein of Salmonella Typhimurium Is Bound Solely by Hydrogen Bonds. *Nature* **1985,** *314*, 257-260.
3. Luecke, H.; Quiocho, F. A. High Specificity of a Phosphate Transport Protein Determined by Hydrogen Bonds. *Nature* **1990,** *347*, 402-406.
4. Koropatkin, N. M.; Pakrasi, H. B.; Smith, T. J. Atomic Structure of a Nitrate-Binding Protein Crucial for Photosynthetic Productivity. *Proc. Nat. Acad. Sci., USA* **2006,** *103*, 9820-9825.
5. Koropatkin, N. M.; Koppenaal, D. W.; Pakrasi, H. B.; Smith, T. J. The Structure of a Cyanobacterial Bicarbonate Transport Protein, Cmpa. *J. Biol. Chem.* **2007,** *282*, 2606-2614.
6. Ihm, H.; Yun, S.; Kim, H. G.; Kim, J. K.; Kim, K. S. Tripodal Nitro-Imidazolium Receptor for Anion Binding Driven by (C−H)+- - -X- Hydrogen Bonds. *Org. Lett.* **2002,** *4*, 2897-2900.
7. Zurro, M.; Asmus, S.; Bamberger, J.; Beckendorf, S.; García Mancheño, O. Chiral Triazoles in Anion-Binding Catalysis: New Entry to Enantioselective Reissert-Type Reactions. *Chem. Eur. J.* **2016,** *22*, 3785-3793.
8. Toure, M.; Charles, L.; Chendo, C.; Viel, S.; Chuzel, O.; Parrain, J.-L. Straightforward and Controlled Shape Access to Efficient Macrocyclic Imidazolylboronium Anion Receptors. *Chem. Eur. J.* **2016,** *22*, 8937-8942.
9. Steed, J. W. Anion-Tuned Supramolecular Gels: A Natural Evolution from Urea Supramolecular Chemistry. *Chem. Soc. Rev.* **2010,** *39*, 3686-3699.
10. Li, A.-F.; Wang, J.-H.; Wang, F.; Jiang, Y.-B. Anion Complexation and Sensing Using Modified Urea and Thiourea-Based Receptors. *Chem. Soc. Rev.* **2010,** *39*, 3729-3745.
11. Zhang, Z.; Schreiner, P. R. (Thio)Urea Organocatalysis-What Can Be Learnt from Anion Recognition? *Chem. Soc. Rev.* **2009,** *38*, 1187-1198.
12. Lizal, T.; Ustrnul, L.; Necas, M.; Sindelar, V. Propanediurea-Based Molecular Clips Bind Halide Anions: An Insight into the Mechanism of Cucurbituril Formation. *J. Org. Chem.* **2016,** *81*, 8906-8910.
13. Allen, F. H.; Lommerse, J. P. M.; Hoy, V. J.; Howard, J. A. K.; Desiraju, G. R. Halogen···O(Nitro) Supramolecular Synthon in Crystal Engineering: A Combined Crystallographic Database and Ab Initio Molecular Orbital Study. *Acta Cryst.* **1997,** *B53*, 1006-1016.
14. Riley, K. E.; Ford Jr, C. L.; Demouchet, K. Comparison of Hydrogen Bonds, Halogen Bonds, CH···Π Interactions, and CX···Π Interactions Using High-Level Ab Initio Methods. *Chem. Phys. Lett.* **2015,** *621*, 165-170.
15. Riley, K. E.; Hobza, P. The Relative Roles of Electrostatics and Dispersion in the Stabilization of Halogen Bonds. *Phys. Chem. Chem. Phys.* **2013,** *15*, 17742-17751.
16. Donoso-Tauda, O.; Jaque, P.; Elguero, J.; Alkorta, I. Traditional and Ion-Pair Halogen-Bonded Complexes between Chlorine and Bromine Derivatives and a Nitrogen-Heterocyclic Carbene. *J. Phys. Chem. A* **2014,** *118*, 9552-9560.
17. Cavallo, G.; Metrangolo, P.; Milani, R.; Pilati, T.; Priimagi, A.; Resnati, G.; Terraneo, G. The Halogen Bond. *Chem. Rev.* **2016,** *116*, 2478-2601.
18. Alkorta, I.; Sanchez-Sanz, G.; Elguero, J.; Bene, J. E. D. FCl:PCX Complexes: Old and New Types of Halogen Bonds. *J. Phys. Chem. A* **2012,** *116*, 2300-2308.
19. Politzer, P.; Murray, J. S. A Unified View of Halogen Bonding, Hydrogen Bonding and Other σ-Hole Interactions. In *Noncovalent Forces*, Scheiner, S., Ed. Springer: Dordrecht, Netherlands, 2015; Vol. 19, pp 357-389.
20. Mele, A.; Metrangolo, P.; Neukirch, H.; Pilati, T.; Resnati, G. A Halogen-Bonding-Based Heteroditopic Receptor for Alkali Metal Halides. *J. Am. Chem. Soc.* **2005,** *127*, 14972-14973.

21. Brown, A.; Beer, P. D. Halogen Bonding Anion Recognition. *Chem. Commun.* **2016,** *52*, 8645-8658.
22. Caballero, A.; Swan, L.; Zapata, F.; Beer, P. D. Iodide-Induced Shuttling of a Halogen- and Hydrogen-Bonding Two-Station Rotaxane. *Angew. Chem. Int. Ed.* **2014,** *53*, 11854-11858.
23. Tepper, R.; Schulze, B.; Jäger, M.; Friebe, C.; Scharf, D. H.; Görls, H.; Schubert, U. S. Anion Receptors Based on Halogen Bonding with Halo-1,2,3-Triazoliums. *J. Org. Chem.* **2015,** *80*, 3139-3150.
24. Barendt, T. A.; Docker, A.; Marques, I.; Félix, V.; Beer, P. D. Selective Nitrate Recognition by a Halogen-Bonding Four-Station [3]Rotaxane Molecular Shuttle. *Angew. Chem. Int. Ed.* **2016,** *55*, 11069-11076.
25. Massena, C. J.; Wageling, N. B.; Decato, D. A.; Martin Rodriguez, E.; Rose, A. M.; Berryman, O. B. A Halogen-Bond-Induced Triple Helicate Encapsulates Iodide. *Angew. Chem. Int. Ed.* **2016,** *55*, 12398-12402.
26. Chudzinski, M. G.; McClary, C. A.; Taylor, M. S. Anion Receptors Composed of Hydrogen- and Halogen-Bond Donor Groups: Modulating Selectivity with Combinations of Distinct Noncovalent Interactions. *J. Am. Chem. Soc.* **2011,** *133*, 10559-10567.
27. Sarwar, M. G.; Dragisic, B.; Dimitrijevic, E.; Taylor, M. S. Halogen Bonding between Anions and Iodoperfluoroorganics: Solution-Phase Thermodynamics and Multidentate-Receptor Design. *Chem. Eur. J.* **2013,** *19*, 2050-2058.
28. Walter, S. M.; Kniep, F.; Rout, L.; Schmidtchen, F. P.; Herdtweck, E.; Huber, S. M. Isothermal Calorimetric Titrations on Charge-Assisted Halogen Bonds: Role of Entropy, Counterions, Solvent, and Temperature. *J. Am. Chem. Soc.* **2012,** *134*, 8507-8512.
29. Borissov, A.; Lim, J. Y. C.; Brown, A.; Christensen, K. E.; Thompson, A. L.; Smith, M. D.; Beer, P. D. Neutral Iodotriazole Foldamers as Tetradentate Halogen Bonding Anion Receptors. *Chem. Commun.* **2017,** *53*, 2483-2486.
30. Tepper, R.; Schulze, B.; Bellstedt, P.; Heidler, J.; Gorls, H.; Jager, M.; Schubert, U. S. Halogen-Bond-Based Cooperative Ion-Pair Recognition by a Crown-Ether-Embedded 5-Iodo-1,2,3-Triazole. *Chem. Commun.* **2017,** *53*, 2260-2263.
31. Dumele, O.; Schreib, B.; Warzok, U.; Trapp, N.; Schalley, C. A.; Diederich, F. Halogen-Bonded Supramolecular Capsules in the Solid State, in Solution, and in the Gas Phase. *Angew. Chem. Int. Ed.* **2017,** *56*, 1152-1157.
32. Wageling, N. B.; Neuhaus, G. F.; Rose, A. M.; Decato, D. A.; Berryman, O. B. Advantages of Organic Halogen Bonding for Halide Recognition. *Supra. Chem.* **2016,** *28*, 665-672.
33. Nepal, B.; Scheiner, S. Competitive Halide Binding by Halogen Versus Hydrogen Bonding: Bis-Triazole Pyridinium. *Chem. Eur. J.* **2015,** *21*, 13330-13335.
34. Nepal, B.; Scheiner, S. Substituent Effects on the Binding of Halides by Neutral and Dicationic Bis(Triazolium) Receptors. *J. Phys. Chem. A* **2015,** *119*, 13064-13073.
35. Nepal, B.; Scheiner, S. Building a Better Halide Receptor: Optimum Choice of Spacer, Binding Unit, and Halosubstitution. *ChemPhysChem.* **2016,** *17*, 836-844.
36. Burling, F. T.; Goldstein, B. M. Computational Studies of Nonbonded Sulfur-Oxygen and Selenium-Oxygen Interactions in the Thiazole and Selenazole Nucleosides. *J. Am. Chem. Soc.* **1992,** *114*, 2313-2320.
37. Iwaoka, M.; Tomoda, S. Nature of the Intramolecular Se···N Nonbonded Interaction of 2-Selenobenzylamine Derivatives. An Experimental Evaluation by ^{1}H, ^{77}Se, and ^{15}N NMR Spectroscopy. *J. Am. Chem. Soc.* **1996,** *118*, 8077-8084.
38. Nagao, Y.; Hirata, T.; Goto, S.; Sano, S.; Kakehi, A.; Iizuka, K.; Shiro, M. Intramolecular Nonbonded S···O Interaction Recognized in (Acylimino)Thiadiazoline Derivatives as Angiotensin II Receptor Antagonists and Related Compounds. *J. Am. Chem. Soc.* **1998,** *120*, 3104-3110.

39. Sánchez-Sanz, G.; Alkorta, I.; Elguero, J. Theoretical Study of the HXYH Dimers (X, Y = O, S, Se). Hydrogen Bonding and Chalcogen–Chalcogen Interactions. *Mol. Phys.* **2011,** *109*, 2543-2552.
40. Adhikari, U.; Scheiner, S. Effects of Charge and Substituent on the S···N Chalcogen Bond. *J. Phys. Chem. A* **2014,** *118*, 3183-3192.
41. Nziko, V. d. P. N.; Scheiner, S. Chalcogen Bonding between Tetravalent SF_4 and Amines. *J. Phys. Chem. A* **2014,** *118*, 10849-10856.
42. Fick, R. J.; Kroner, G. M.; Nepal, B.; Magnani, R.; Horowitz, S.; Houtz, R. L.; Scheiner, S.; Trievel, R. C. Sulfur–Oxygen Chalcogen Bonding Mediates Adomet Recognition in the Lysine Methyltransferase Set7/9. *ACS Chem. Biol.* **2016,** *11*, 748-754.
43. Zhao, H.; Gabbaï, F. P. A Bidentate Lewis Acid with a Telluronium Ion as an Anion-Binding Site. *Nat Chem* **2010,** *2*, 984-990.
44. Garrett, G. E.; Gibson, G. L.; Straus, R. N.; Seferos, D. S.; Taylor, M. S. Chalcogen Bonding in Solution: Interactions of Benzotelluradiazoles with Anionic and Uncharged Lewis Bases. *J. Am. Chem. Soc.* **2015,** *137*, 4126-4133.
45. Garrett, G. E.; Carrera, E. I.; Seferos, D. S.; Taylor, M. S. Anion Recognition by a Bidentate Chalcogen Bond Donor. *Chem. Commun.* **2016,** *52*, 9881-9884.
46. Benz, S.; Macchione, M.; Verolet, Q.; Mareda, J.; Sakai, N.; Matile, S. Anion Transport with Chalcogen Bonds. *J. Am. Chem. Soc.* **2016,** *138*, 9093-9096.
47. Lim, J. Y. C.; Marques, I.; Thompson, A. L.; Christensen, K. E.; Félix, V.; Beer, P. D. Chalcogen Bonding Macrocycles and [2]Rotaxanes for Anion Recognition. *J. Am. Chem. Soc.* **2017,** *139*, 3122-3133.
48. Moilanen, J.; Ganesamoorthy, C.; Balakrishna, M. S.; Tuononen, H. M. Weak Interactions between Trivalent Pnictogen Centers: Computational Analysis of Bonding in Dimers $X_3E{\cdots}EX_3$ (E = Pnictogen, X = Halogen). *Inorg. Chem.* **2009,** *48*, 6740-6747.
49. Scheiner, S. Can Two Trivalent N Atoms Engage in a Direct N···N Noncovalent Interaction? *Chem. Phys. Lett.* **2011,** *514*, 32-35.
50. Bene, J. E. D.; Alkorta, I.; Sanchez-Sanz, G.; Elguero, J. Structures, Energies, Bonding, and NMR Properties of Pnicogen Complexes $H_2XP{:}NXH_2$ (X = H, CH_3, NH_2, OH, F, Cl). *J. Phys. Chem. A* **2011,** *115*, 13724-13731.
51. Scheiner, S. Effects of Multiple Substitution Upon the P···N Noncovalent Interaction. *Chem. Phys.* **2011,** *387*, 79-84.
52. Li, Q.-Z.; Li, R.; Liu, X.-F.; Li, W.-Z.; Cheng, J.-B. Concerted Interaction between Pnicogen and Halogen Bonds in $XCl\text{-}FH_2P\text{-}NH_3$ (X=F, OH, CN, NC, and FCC). *ChemPhysChem.* **2012,** *13*, 1205-1212.
53. Scheiner, S. The Pnicogen Bond: Its Relation to Hydrogen, Halogen, and Other Noncovalent Bonds. *Acc. Chem. Res.* **2013,** *46*, 280-288.
54. Scheiner, S. Detailed Comparison of the Pnicogen Bond with Chalcogen, Halogen and Hydrogen Bonds. *Int. J. Quantum Chem.* **2013,** *113*, 1609-1620.
55. Bauzá, A.; Mooibroek, T. J.; Frontera, A. Σ-Hole Opposite to a Lone Pair: Unconventional Pnicogen Bonding Interactions between ZF_3 (Z=N, P, As, and Sb) Compounds and Several Donors. *ChemPhysChem.* **2016,** *17*, 1608-1614.
56. Scheiner, S.; Adhikari, U. Abilities of Different Electron Donors (D) to Engage in a P···D Noncovalent Interaction. *J. Phys. Chem. A* **2011,** *115*, 11101-11110.
57. Bauzá, A.; Ramis, R.; Frontera, A. Computational Study of Anion Recognition Based on Tetrel and Hydrogen Bonding Interaction by Calix[4]Pyrrole Derivatives. *Comput. Theor. Chem.* **2014,** *1038*, 67-70.
58. Grabowski, S. J. Tetrel Bond–σ-Hole Bond as a Preliminary Stage of the S_n2 Reaction. *Phys. Chem. Chem. Phys.* **2014,** *16*, 1824-1834.

59. Tang, Q.; Li, Q. Interplay between Tetrel Bonding and Hydrogen Bonding Interactions in Complexes Involving F_2XO (X=C and Si) and HCN. *Comput. Theor. Chem.* **2014,** *1050*, 51-57.
60. Azofra, L. M.; Scheiner, S. Tetrel, Chalcogen, and CH···O Hydrogen Bonds in Complexes Pairing Carbonyl-Containing Molecules with 1, 2, and 3 Molecules of CO_2. *J. Chem. Phys.* **2015,** *142*, 034307.
61. Scheiner, S. Comparison of CH···O, SH···O, Chalcogen, and Tetrel Bonds Formed by Neutral and Cationic Sulfur-Containing Compounds. *J. Phys. Chem. A* **2015,** *119*, 9189-9199.
62. Del Bene, J. E.; Alkorta, I.; Elguero, J. Exploring the $(H_2C{=}PH_2)^+$:N-Base Potential Surfaces: Complexes Stabilized by Pnicogen, Hydrogen, and Tetrel Bonds. *J. Phys. Chem. A* **2015,** *119*, 11701-11710.
63. Southern, S. A.; Bryce, D. L. NMR Investigations of Noncovalent Carbon Tetrel Bonds. Computational Assessment and Initial Experimental Observation. *J. Phys. Chem. A* **2015,** *119*, 11891-11899.
64. Marín-Luna, M.; Alkorta, I.; Elguero, J. A Theoretical Study of the $H_nf_{4-N}si$:N-Base (n = 1–4) Tetrel-Bonded Complexes. *Theor. Chem. Acc.* **2017,** *136*, 41-.
65. Liu, M.; Li, Q.; Scheiner, S. Comparison of Tetrel Bonds in Neutral and Protonated Complexes of Pyridinetf_3 and Furantf_3 (T = C, Si, and Ge) with NH_3. *Phys. Chem. Chem. Phys.* **2017,** *19*, 5550-5559.
66. Scheiner, S. Highly Selective Halide Receptors Based on Chalcogen, Pnicogen, and Tetrel Bonds. *Chem. Eur. J.* **2016,** *22*, 18850-18858.
67. Scheiner, S. Comparison of Halide Receptors Based on H, Halogen, Chalcogen, Pnicogen, and Tetrel Bonds. *Faraday Discuss. Chem. Soc.* **2017**, in press. DOI: 10.1039/C7FD00043J
68. Walter, S. M.; Kniep, F.; Herdtweck, E.; Huber, S. M. Halogen-Bond-Induced Activation of a Carbon–Heteroatom Bond. *Angew. Chem. Int. Ed.* **2011,** *50*, 7187-7191.
69. Sabater, P.; Zapata, F.; Caballero, A.; de la Visitación, N.; Alkorta, I.; Elguero, J.; Molina, P. Comparative Study of Charge-Assisted Hydrogen- and Halogen-Bonding Capabilities in Solution of Two-Armed Imidazolium Receptors toward Oxoanions. *J. Org. Chem.* **2016,** *81*, 7448-7458.
70. Chakraborty, S.; Dutta, R.; Ghosh, P. Halogen Bonding Assisted Selective Removal of Bromide. *Chem. Commun.* **2015,** *51*, 14793-14796.
71. Zapata, F.; Caballero, A.; White, N. G.; Claridge, T. D. W.; Costa, P. J.; Félix, V.; Beer, P. D. Fluorescent Charge-Assisted Halogen-Bonding Macrocyclic Halo-Imidazolium Receptors for Anion Recognition and Sensing in Aqueous Media. *J. Am. Chem. Soc.* **2012,** *134*, 11533-11541.
72. Zhao, Y.; Truhlar, D. G. The M06 Suite of Density Functionals for Main Group Thermochemistry, Thermochemical Kinetics, Noncovalent Interactions, Excited States, and Transition Elements: Two New Functionals and Systematic Testing of Four M06-Class Functionals and 12 Other Functionals. *Theor. Chem. Acc.* **2008,** *120*, 215-241.
73. Frisch, M. J.; Trucks, G. W.; Schlegel, H. B.; Scuseria, G. E.; Robb, M. A.; Cheeseman, J. R.; Scalmani, G.; Barone, V.; Mennucci, B.; Petersson, G. A., et al. *Gaussian 09*, Revision B.01; Wallingford, CT, 2009.
74. Feller, D. The Role of Databases in Support of Computational Chemistry Calculations. *J. Comput. Chem.* **1996,** *17*, 1571-1586.
75. Schuchardt, K. L.; Didier, B. T.; Elsethagen, T.; Sun, L.; Gurumoorthi, V.; Chase, J.; Li, J.; Windus, T. L. Basis Set Exchange: A Community Database for Computational Sciences. *J. Chem. Infor. Model.* **2007,** *47*, 1045-1052.
76. Boese, A. D. Density Functional Theory and Hydrogen Bonds: Are We There Yet? *ChemPhysChem.* **2015,** *16*, 978-985.
77. Sladek, V.; Škorňa, P.; Poliak, P.; Lukeš, V. The Ab Initio Study of Halogen and Hydrogen Σ_n-Bonded Para-Substituted Pyridine···(X_2/XY/HX) Complexes. *Chem. Phys. Lett.* **2015,** *619*, 7-13.

78. Li, A.; Muddana, H. S.; Gilson, M. K. Quantum Mechanical Calculation of Noncovalent Interactions: A Large-Scale Evaluation of Pmx, DFT, and SAPT Approaches. *J. Chem. Theory Comput.* **2014,** *10*, 1563-1575.
79. Forni, A.; Pieraccini, S.; Rendine, S.; Sironi, M. Halogen Bonds with Benzene: An Assessment of DFT Functionals. *J. Comput. Chem.* **2014,** *35*, 386-394.
80. Bauzá, A.; Alkorta, I.; Frontera, A.; Elguero, J. On the Reliability of Pure and Hybrid DFT Methods for the Evaluation of Halogen, Chalcogen, and Pnicogen Bonds Involving Anionic and Neutral Electron Donors. *J. Chem. Theory Comput.* **2013,** *9*, 5201-5210.
81. Walker, M.; Harvey, A. J. A.; Sen, A.; Dessent, C. E. H. Performance of M06, M06-2x, and M06-HF Density Functionals for Conformationally Flexible Anionic Clusters: M06 Functionals Perform Better Than B3LYP for a Model System with Dispersion and Ionic Hydrogen-Bonding Interactions. *J. Phys. Chem. A* **2013,** *117*, 12590-12600.
82. Mardirossian, N.; Head-Gordon, M. Characterizing and Understanding the Remarkably Slow Basis Set Convergence of Several Minnesota Density Functionals for Intermolecular Interaction Energies. *J. Chem. Theory Comput.* **2013,** *9*, 4453–4461.
83. Elm, J.; Bildeb, M.; Mikkelsena, K. V. Assessment of Binding Energies of Atmospherically Relevant Clusters. *Phys. Chem. Chem. Phys.* **2013,** *15*, 16442-16445.
84. DiLabio, G. A.; Johnson, E. R.; Otero-de-la-Roza, A. Performance of Conventional and Dispersion-Corrected Density-Functional Theory Methods for Hydrogen Bonding Interaction Energies. *Phys. Chem. Chem. Phys.* **2013,** *15*, 12821-12828.
85. Rosokha, S. V.; Stern, C. L.; Ritzert, J. T. Experimental and Computational Probes of the Nature of Halogen Bonding: Complexes of Bromine-Containing Molecules with Bromide Anions. *Chem. Eur. J.* **2013,** *19*, 8774-8788.
86. Boys, S. F.; Bernardi, F. The Calculation of Small Molecular Interactions by the Differences of Separate Total Energies. Some Procedures with Reduced Errors. *Mol. Phys.* **1970,** *19*, 553-566.
87. Barone, V.; Cossi, M. Quantum Calculation of Molecular Energies and Energy Gradients in Solution by a Conductor Solvent Model. *J. Phys. Chem. A* **1998,** *102*, 1995-2001.
88. Zhurko, G. A. *Chemcraft*.
89. Bulat, F. A.; Toro-Labbé, A.; Brinck, T.; Murray, J. S.; Politzer, P. Quantitative Analysis of Molecular Surfaces: Areas, Volumes, Electrostatic Potentials and Average Local Ionization Energies. *J. Mol. Model.* **2010,** *16*, 1679-1691.
90. Glendening, E. D.; Landis, C. R.; Weinhold, F. NBO 6.0: Natural Bond Orbital Analysis Program. *J. Comput. Chem.* **2013,** *34*, 1429-1437.
91. Iyer, S.; Lopez-Hilfiker, F.; Lee, B. H.; Thornton, J. A.; Kurtén, T. Modeling the Detection of Organic and Inorganic Compounds Using Iodide-Based Chemical Ionization. *J. Phys. Chem. A* **2016,** *120*, 576-587.

Table 1. Binding energies (kcal/mol) in the gas phase

		R=H	R=I	R=SnH_3	R=SiF_3
Im-R^+	F^-	130.09	126.01	142.06	175.13
	Cl^-	25.08	28.38	38.08	52.13
R-Im-Bz-Im-R^{+2}	F^-	196.57	191.17	206.14	231.65
	Cl^-	97.89	93.45	99.08	106.62
R-ImF-Bz-ImF-R^{+2}	F^-	212.86	202.44	216.83	242.79
	Cl^-	104.90	104.19	109.33	124.88
R-ImF_3-Bz-ImF_3-R^{+2}	F^-	221.16	209.58	223.88	251.50
	Cl^-	110.77	111.17	116.07	127.57

Table 2. Binding energies (kcal/mol) in aqueous solution

		R=H	R=I	R=SnH_3	R=SiF_3
Im-R^+	F^-	7.03	14.14	24.34	53.80
	Cl^-	0.99	3.03	4.82	15.22
R-Im-Bz-Im-R^{+2}	F^-	17.37	22.77	29.84	51.92
	Cl^-	8.59	12.55	10.18	11.00
R-ImF-Bz-ImF-R^{+2}	F^-	24.16	27.74	35.73	59.04
	Cl^-	9.70	16.09	14.83	18.38
R-ImF_3-Bz-ImF_3-R^{+2}	F^-	29.46	31.98	40.78	63.87
	Cl^-	10.67	19.37	19.07	23.34

Table 3. Advantage in binding free energy (kcal/mol) at 298 K of F^- over Cl^-, and equilibrium ratio K for preference of F^- over Cl^- in aqueous solution.

		R=H	R=I	R=SnH_3	R=SiF_3
Im-R^+	ΔG	8.70	10.10	19.02	36.90
	K	2.4E+06	2.5E+07	8.5E+13	1.1E+27
R-Im-Bz-Im-R^{+2}	ΔG	10.08	9.42	18.36	40.15
	K	2.4E+07	7.9E+06	2.8E+13	2.6E+29
R-ImF-Bz-ImF-R^{+2}	ΔG	15.86	11.05	20.10	39.37
	K	4.1E+11	1.2E+08	5.3E+14	6.8E+28
R-ImF_3-Bz-ImF_3-R^{+2}	ΔG	20.09	11.81	20.11	38.93
	K	5.1E+14	4.4E+08	5.3E+14	3.2E+28

Table 4. NBO $X_{lp} \rightarrow \sigma^*$(R-C) charge transfer energy E(2) (kcal/mol) and electron density at AIM X••R bond critical point (au)

		NBO E(2)				ρ_{BCP}			
		R=H	R=I	R=SnH_3	R=SiF_3	R=H	R=I	R=SnH_3	R=SiF_3
Im-R^+	F^-	[a,b]	101.8	78.81	5.13	0.2718	0.0895	0.0910	0.1102
	Cl^-	59.92	91.49	[b]	8.85	0.0588	0.0588	0.0590	0.0826
R-Im-Bz-Im-R^{+2}	F^-	53.51	37.31	[b]	[b]	0.0617	0.0524	0.0542	0.0699
	Cl^-	31.41	36.99	44.12	4.60	0.0307	0.0372	0.0364	0.0547
R-ImF-Bz-ImF-R^{+2}	F^-	12.21[a]	41.50	[b]	37.92	0.0228[a]	0.0553	0.0572	0.0707
	Cl^-	43.52	44.12	[b]	4.59	0.0379	0.0408	0.0385	0.0573
R-ImF_3-Bz-ImF_3-R^{+2}	F^-	12.56[a]	44.84	[b]	42.11	0.0235[a]	0.0565	0.0582	0.0707
	Cl^-	50.22	47.59	[b]	4.65	0.0420	0.0426	0.0397	0.0580

[a]R at least partially transferred to X^-

[b]NBO unable to make proper separation of subunits

Table 5. $V_{s,max}$ (kcal/mol)

	R=H	R=I	R=SnH_3	R=SiF_3
Im-R^+	124.31	110.91	117.88	123.54
R-Im-Bz-Im-R^{+2}	174.56	152.38	159.64	170.75
R-ImF-Bz-ImF-R^{+2}	186.34	161.96	168.46	181.27
R-ImF_3-Bz-ImF_3-R^{+2}	213.67[a]	167.32	174.30	187.34

[a]used geometry of complex with Cl^-

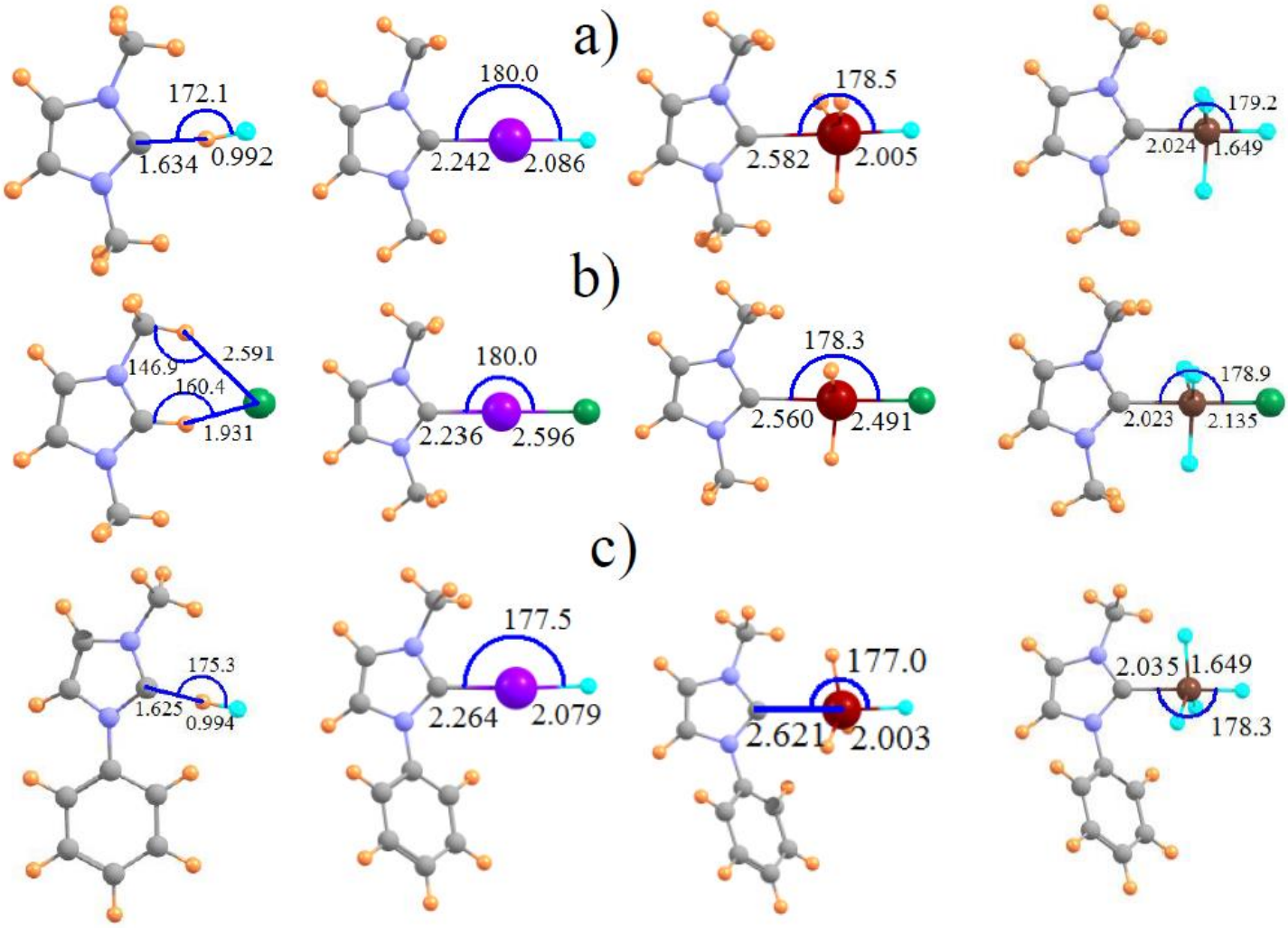

Fig 1. Optimized geometries of complexes of a) F^- and b) Cl^- with ImH^+ and its I, SnH_3, and SiF_3-substituted derivatives. c) Complexes of F^- with phenyl-substituted receptors. Distances in Å and angles in degs.

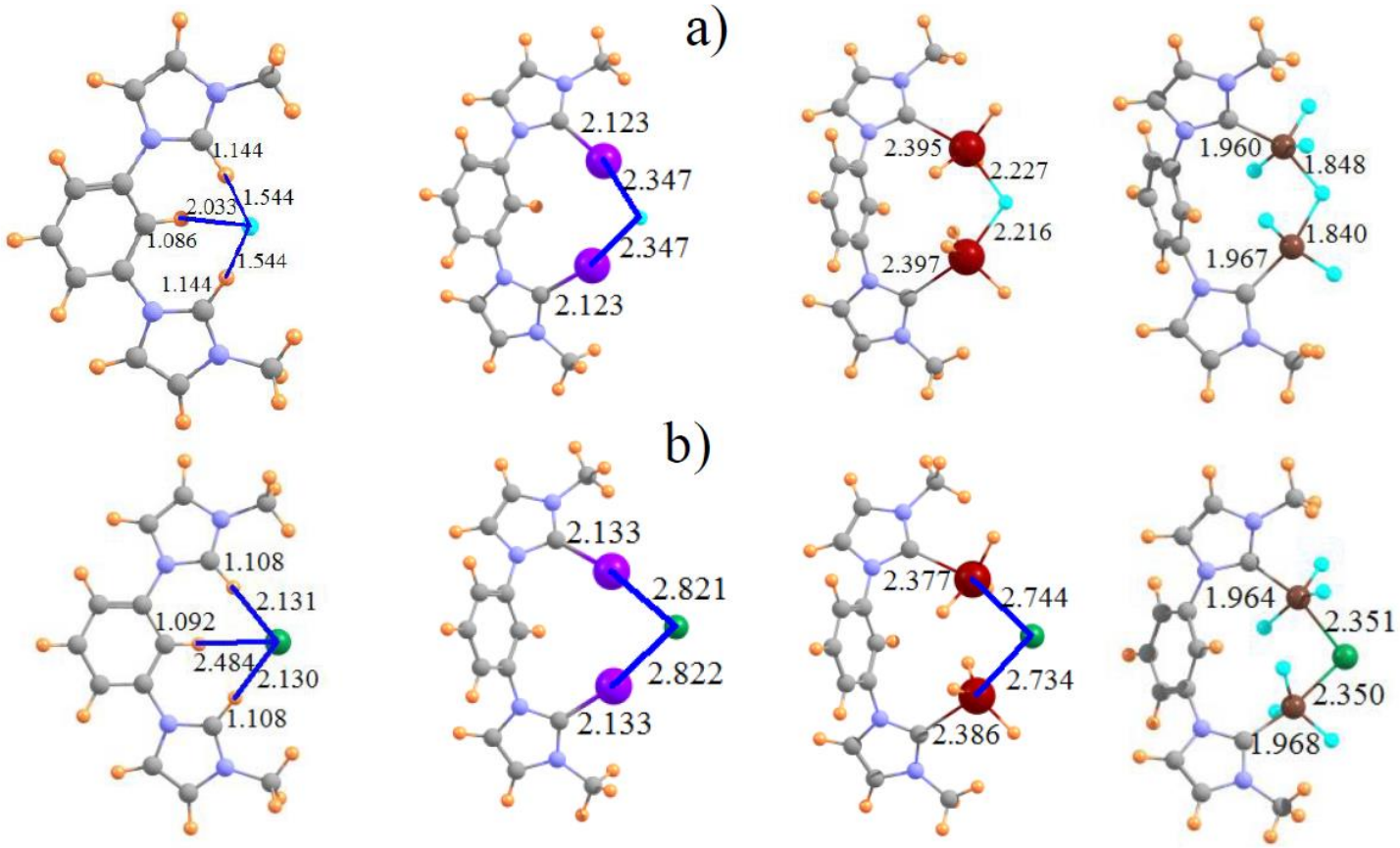

Fig 2. Optimized geometries of complexes of a) F^- and b) Cl^- with R-Im-Bz-Im-R^{+2}, R=H, I, SnH_3, and SiF_3. Distances in Å.

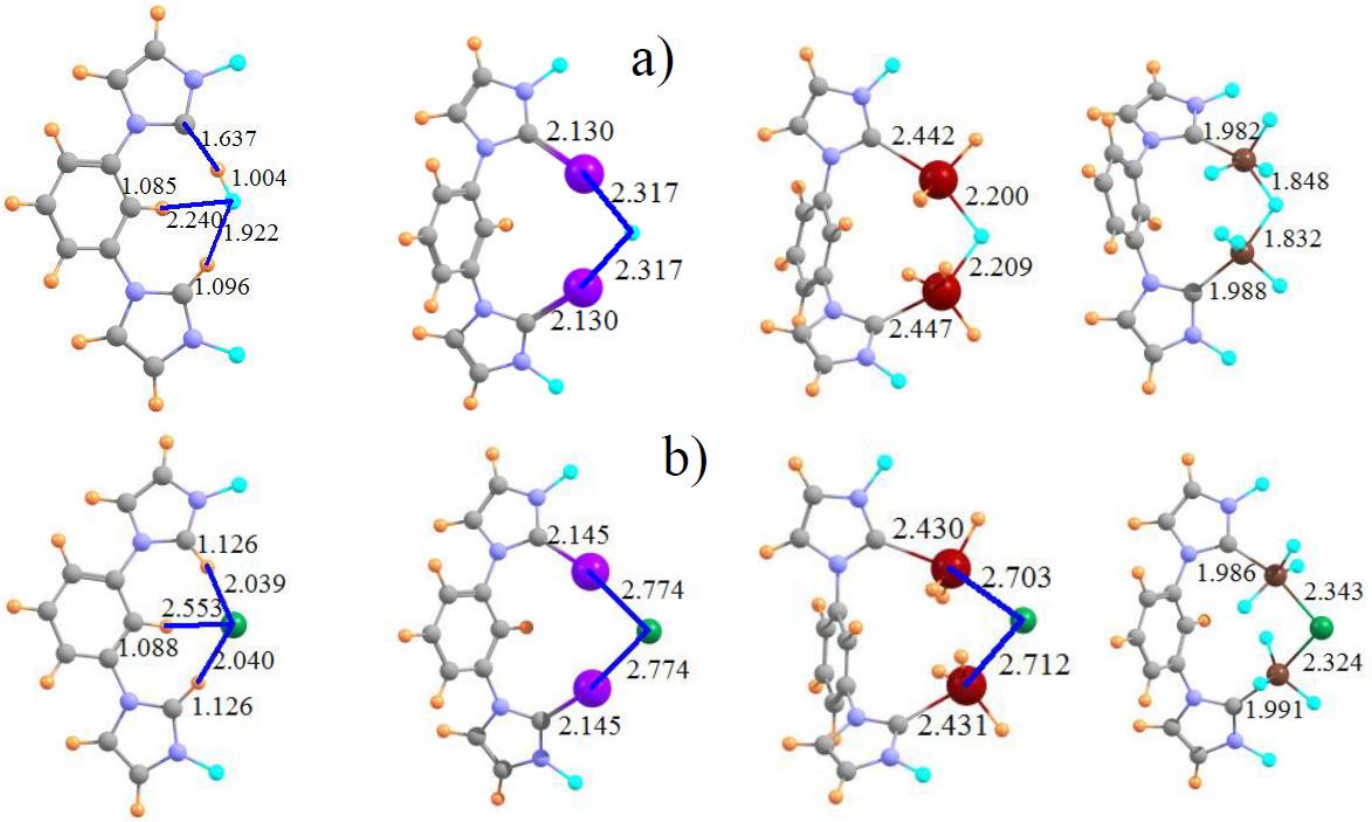

Fig 3. Optimized geometries of complexes of a) F^- and b) Cl^- with R-ImF-Bz-ImF-R^{+2}, R=H, I, SnH_3, and SiF_3. Distances in Å.

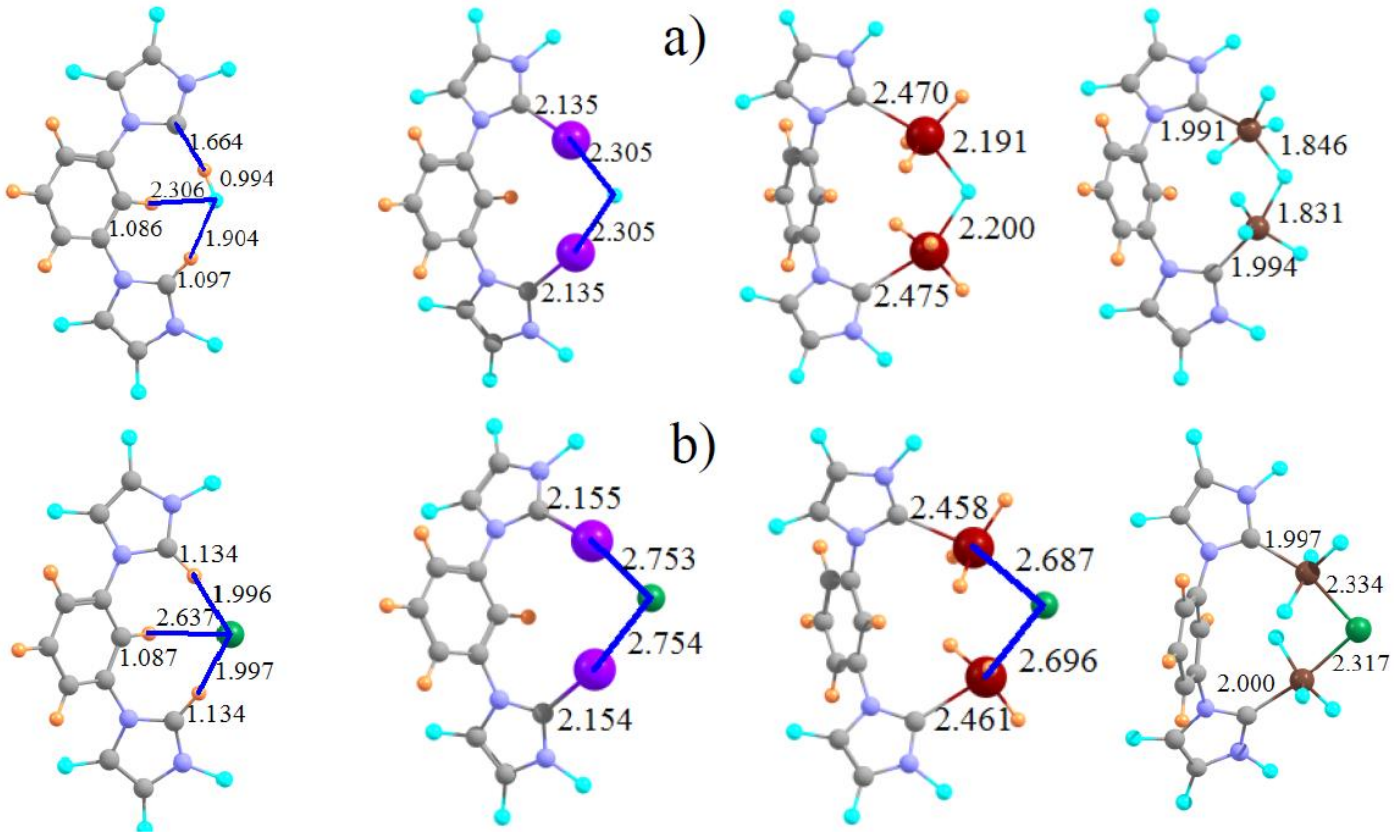

Fig 4. Optimized geometries of complexes of a) F^- and b) Cl^- with R-ImF_3-Bz-ImF_3-R^{+2}, R=H, I, SnH_3, and SiF_3. Distances in Å.

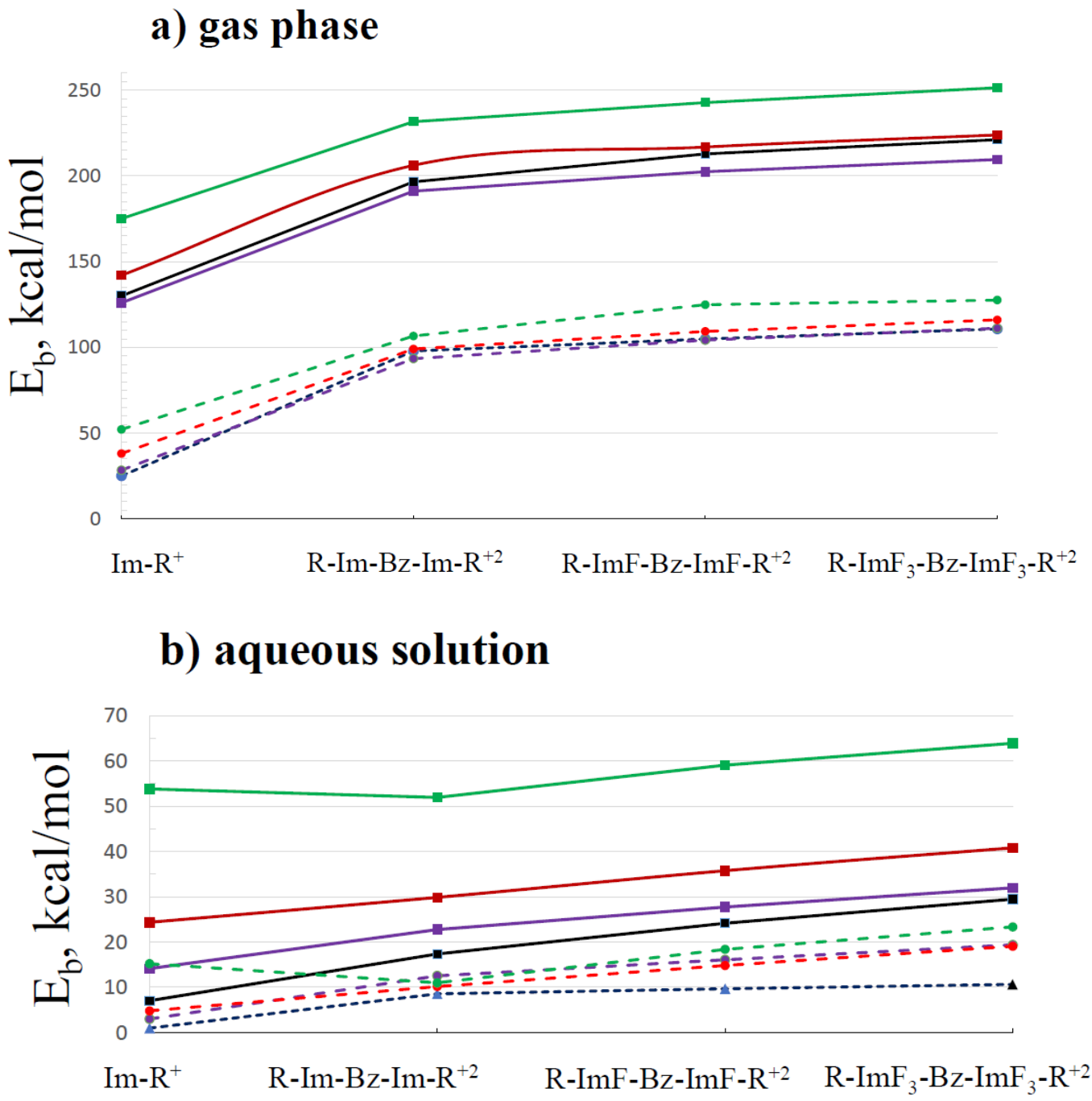

Fig 5. Binding energies of F^- (solid lines) and Cl^- (broken lines) with indicated receptors. Black lines refer to R=H, purple to R=I, red to R= SnH_3, and green to R=SiF_3. Gas phase values shown in a and aqueous solution in b.

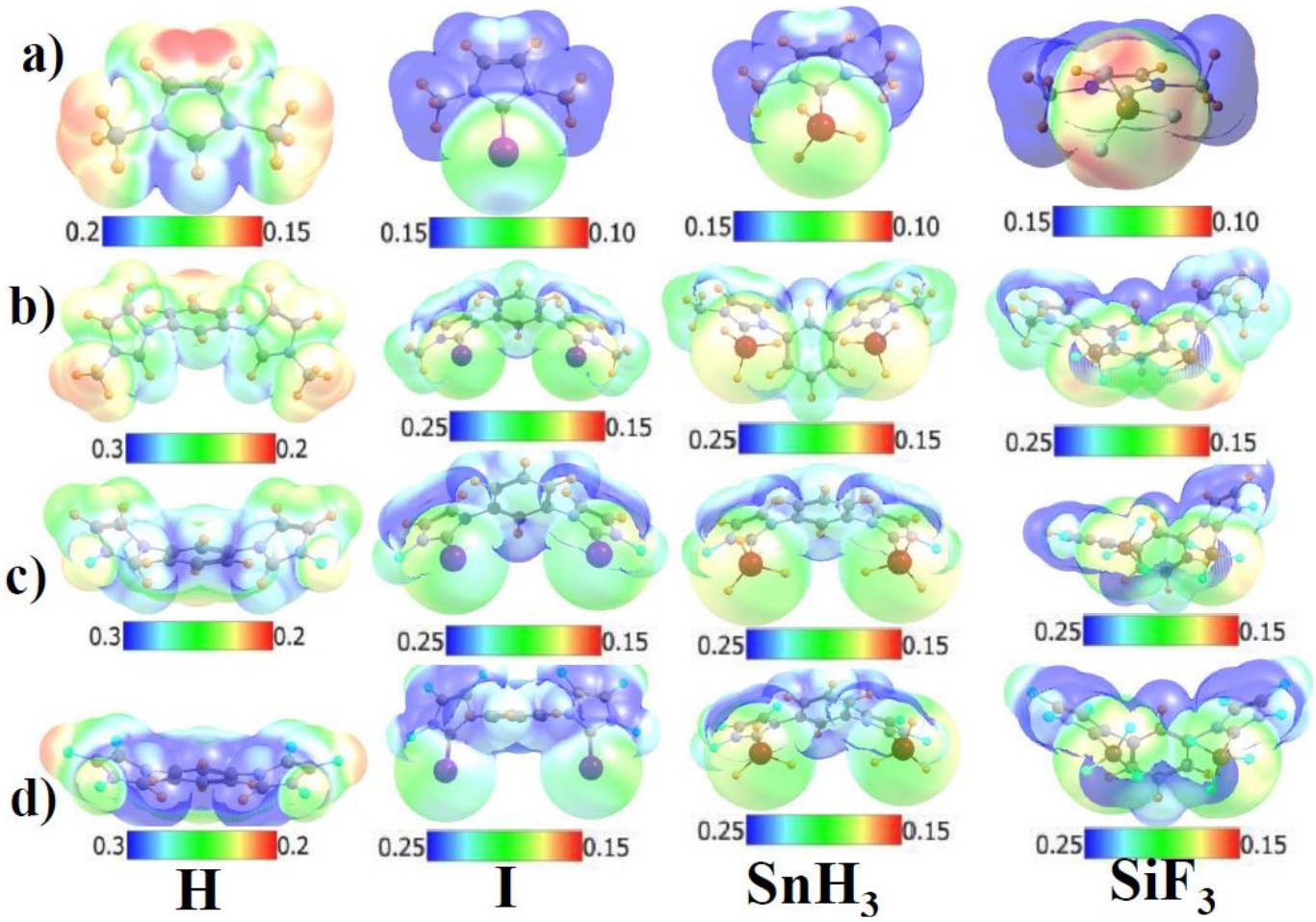

Fig 6. Molecular electrostatic potentials (MEPs) of receptors, illustrated on a surface corresponding to 1.5 times the vdW radius of each atom. a) ImR^{+}, b) R-Im-Bz-Im-R^{+2}, c) R-ImF-Bz-ImF-R^{+2}, d) R-ImF_3-Bz-ImF_3-R^{+2}. Ranges shown are in au.

Table of Contents Graphic